Semiconductor device modeling with SCAPS-1D

Lecture 4

Special Topics:
Device Modeling

Outline

- Basic concepts and physics model
- Overview of capabilities
- Input/Output
- Brief literature survey of problems/results
- Hands on: running standard models, creating a simple model

SCAPS-1D

- SCAPS (a Solar Cell Capacitance Simulator) is a one-dimensional solar cell simulation program
- Developed at the Department of Electronics and Information Systems (ELIS) of the University of Gent, Belgium
- The program is freely available to the research community (reference it in your publications)
- Continuously supported and further developed (http://scaps.elis.ugent.be); runs under Windows

SCAPS-1D

- Originally developed for polycrystalline cell structures of the $CuInSe_2$ and the CdTe family
  - Basis reference paper published in 2000
- Designed to accommodate thin films, multiple interfaces, large band gaps (Eg=1.12eV for Si, but 2.4eV for CdS used as window layer)
- The package evolved over the years to include additional mechanisms, e.g., Auger recombination, tunneling, multiple enhancement to user interface, etc.

Device model

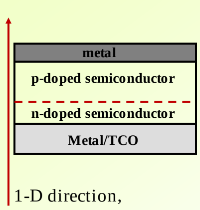

1-D direction, *x* coordinate

- Device is modeled in one dimension across layers, and formed junctions in physical space
- Depth is *x* coordinate
- Spatial distributions of fields, charge carriers, defects, etc.

Device model: energy space

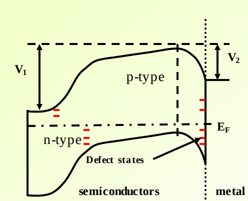

- Band diagram of a realistic p-n heterojunction with back barrier and defect states at thermodynamic equilibrium
- Compared to AMPS: better description of recombination processes; several tunneling mechanisms are included in SCAPS

Physics model: governing equations

- The Poisson equation, and the continuity equations for electrons and holes (same as in AMPS-1D)

$$\frac{\partial}{\partial x}\left(\varepsilon(x)\frac{\partial \psi}{\partial x}\right) = -\frac{q}{\varepsilon_0}\cdot\left[-n + p - N_A^- + N_D^+ + \frac{1}{q}\rho_{def}(n,p)\right]$$

$$-\frac{\partial j_n}{\partial x} + G - U_n(n,p) = \frac{\partial n}{\partial t}$$

$$-\frac{\partial j_p}{\partial x} + G - U_p(n,p) = \frac{\partial p}{\partial t}$$

p,*n* – free carrier concentrations
$N^{\pm}_{DA}$ – charged dopants
ρ_{def}(n,p) – defect distributions
j_n, j_p – the electron and hole current densities
$U_{n,p}$ - the net recombination rates;
G - the generation rate

Physics model: solving governing equations

- Constitutive relations

$$j_n = -\frac{\mu_n}{q}\frac{\partial E_{Fn}}{\partial x}; \qquad j_p = -\frac{\mu_p}{q}\frac{\partial E_{Fp}}{\partial x}$$

- Solve for potential and quasi-Fermi levels
- Boundary conditions at interfaces and contacts
- Structure is discretized, meshing refined around interfaces
- Newton-Raphson method with algorithm modifications

Physics model: interfaces

- The quasi-fermi levels are allowed to be discontinuous at the interfaces
- Recombination at the interface states is handled

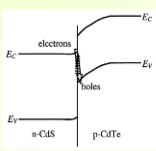

Example: recombination between electrons of CdS and holes in the CdTe on the right side of the interface

Physics model: grading

- Almost all parameters can be graded; the principles of the algorithms used to simulate graded solar cell structures
- All parameters are consistently derived from the composition grading of a layer
  – Each layer is assumed to have composition $A_{1-y}B_y$
  – Define values of a parameter P for pure compounds A, B, and the composition grading $y(x)$ over the layer thickness
  – Specify some grading law for $P(y)$

Physics model: grading

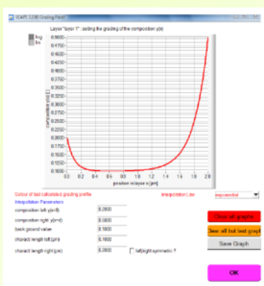

- Grading laws: uniform, linear, exponential, etc.
- Alternatively, the composition grading profile can be loaded from a file

Physics model: generation

- From internal calculation under illumination
  – Dark or light, power level (~ND filter), choice of the illuminated side, choice of the spectrum
- From user supplied generation g(x) file, at the *x*-coordinates of the nodes used by SCAPS
  – allows for modeling of radiation detectors, EBIC measurements
  – Solar cell efficiency and QE cannot be calculated; may use collection efficiency, based on "ideal" device current

Physics model: recombination

- Direct band-to-band
  - Between the occupied states in the CB and the vacant states in the VB
- Indirect, or Shockley-Read-Hall
  - Through a defect state in the gap
  - Also through interface states
- Auger recombination
  - Involves three carriers: after recombination, the energy is given an electron in the conduction band (as opposed to emission as a photon or phonon)

Physics model: tunneling

- The following tunneling mechanisms are treated: band to band tunneling, intraband tunneling, tunneling to interface defects and tunneling to contacts

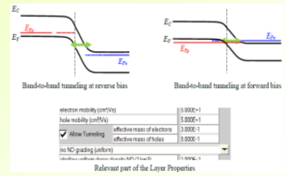

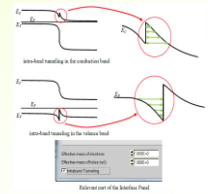

Physics model: tunneling

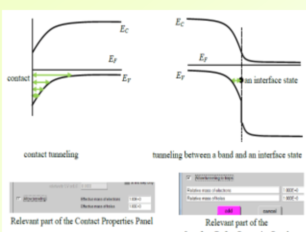

- Tunneling is only taken into account in the solution of the dc-problem
- Only indirect tunnel influences on the admittance (through the setting of the dc-state of the sample)

Input: action panel

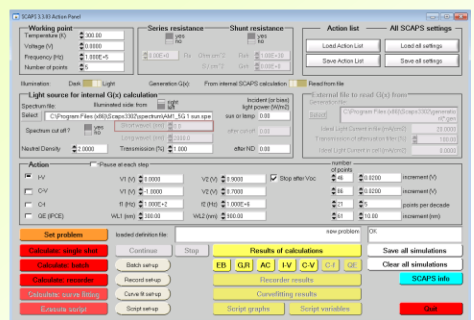

Output

- In each calculation the running parameter (V, f, or λ) is varied in the specified range
- Plot all calculated parameters, such as I/V, C/V, C/f, Q(λ), band diagrams, concentrations, and currents
- All calculations can be saved in ASCII format
- When divergence occurs, the points calculated so far are shown on the corresponding graphs
- Batch calculations possible; presentation of results and settings as a function of batch parameters

Device definition

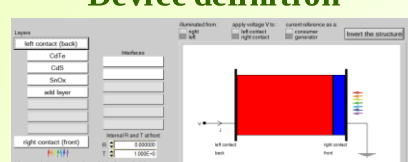

- Device is represented as a stack of layers, up to 7 semiconductor layers with specified properties
- Separate entries for interface parameters
- Two additional layers for contacts, front and back

Quantum efficiency

- The Q.E. is the ratio of the number of carriers collected by the solar cell to the number of photons of a given energy incident on the solar cell
- If all photons of a certain wavelength are absorbed and the resulting minority carriers are collected, then the quantum efficiency at that particular wavelength is unity
- The quantum efficiency for photons with energy below the band gap is zero

Quantum efficiency

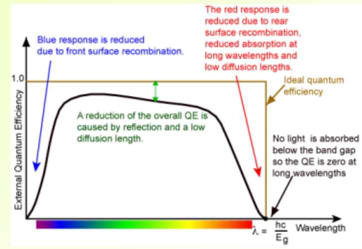

Image from ASU PV education website
http://www.pveducation.org/pvcdrom/solar-cell-operation/quantum-efficiency

Admittance spectroscopy

- Small signal analysis, C(V) of C(f)
- The cell structure is analyzed as if it were a parallel connection of a (frequency dependent) capacitance and a (frequency dependent) conductance

$$Y(\omega) = \frac{\tilde{J}}{\tilde{u}_{ext}} = i\omega C(\omega) + G(\omega)$$

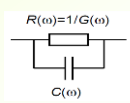

T. Walter, R. Herberholz, C. Müller, H.W. Schock, *Determination of defect distributions from admittance measurements and application to Cu(In,Ga)Se₂ based heterojunctions*, Journal of Applied Physics, 80 (1996) 4411-4420.
K. Decock, S. Khelifi, S. Buecheler, F. Pianezzi, A.N. Tiwari, M. Burgelman, *Defect distributions in thin film solar cells deduced from admittance measurements under different bias voltages*, Journal of Applied Physics, 110 (2011) 063722

Admittance spectroscopy

- The C–V profiling tests the spatial charge distribution ($1/C^2$ vs V gives total defect + dopants concentration)
- Frequency dependent admittance $Y(\omega)$ is generally attributed to defects

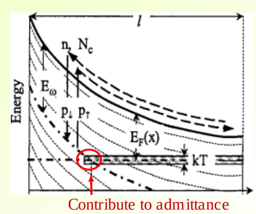

- In response to the small testing ac electric potential, defects change their occupation numbers depending on their relaxation times
- Changing ω (and $E_\omega = kT\ln(\omega\tau_0)$) – scan energies of resonant states
- Changing bias and bend bending – scan along distance from CB

Output

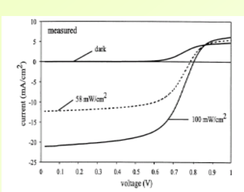

Fig. 5. Measured *I–V* curves of a CdS/CdTe/Au solar cell, for varying illumination intensity.

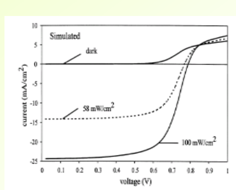

Fig. 6. SCAPS simulation of the *I–V* curves of a CdS/CdTe/Au solar cell, for varying illumination intensity.

From standard I-V curves at different levels of illumination

Output

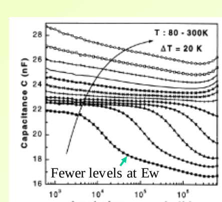

Fig. 9. Measured *C–f* curves of a CIGS solar cell in the temperature range 80–300 K (20 K steps).

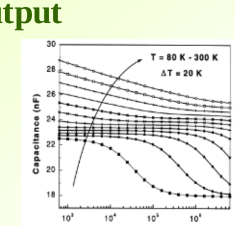

Fig. 10. SCAPS simulation of *C–f* curves of a CIGS solar cell in the temperature range 80–300 K (20 K steps).

To temperature-dependent admittance spectroscopy (C/f)

Data analysis features

- Data analysis is supported within the package: any ASCII-text file can be read as a measurement file
  - The file extension indicates which kind of measurement it contains: '.iv', '.cv', '.cf' or '.qe'
- A built-in curve fitting facility
- Quantum efficiency panel
- A panel for the interpretation of admittance measurements (C/f and C/V)

SCAPS-1D

BRIEF LITERATURE SURVEY OF PROBLEMS AND RESULTS

Analysis of graded band gap solar cells with SCAPS

M. Burgelman and J. Marleinthin, 23rd European PV Conference, Valencia, Spain, 2008

- In $Cu(In,Ga)(Se,S)_2$ devices the absorber materials are engineered to have an optimized band gap energy *Eg* (trade-off between high current for low *Eg* and high voltage for high *Eg*)

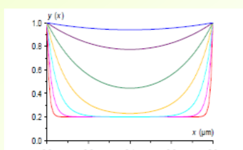

Fig. 4 Composition grading $y(x)$ of the CIGS layer used in the simulations of Fig. 5 and Fig. 6. The profile is 'exponential' with $y_{left} = y_{right} = 1$, $y_0 = 0.2$. The characteristic length L is logarithmically varying in 7 steps from 0.01 µm (red) to 1.00 µm (blue).

Analysis of graded band gap solar cells with SCAPS

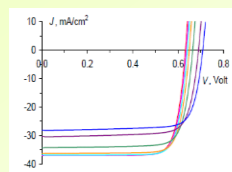

Fig. 5 SCAPS *I-V* simulation of cells with a graded CIGS layer. The composition profiles $y(x)$ of the different curves is as in Fig. 4, with the same colour code.

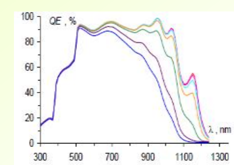

Fig. 6 SCAPS *QE* simulation of cells with a graded CIGS layer. The composition profiles $y(x)$ of the different curves is as in Fig. 4, with the same colour code.

Ga- content should be low over most of the CIGS bulk, but high in a narrow region at the back contact and at the interface; a characteristic width < 50 nm seems to be sufficient to combine high *Jsc* with high *Voc*

Advanced electrical simulation of thin film solar cells

M. Burgelman, K. Decock, S. Khelifi and A. Abass, Thin Solid Films, 535 (2013) 296-301

- The result of measurements performed on CIGS based solar cells depends on history of the sample
- The model includes band gap grading, multivalent defects and metastable transitions between defects
  - The occupation of metastable defects is set during initial conditions at higher temperature, and then frozen in during cell operation at lower temperature
  - Metastable states of the double vacancy type (V_{Se}–V_{Cu}) were introduced

Advanced electrical simulation of thin film solar cells

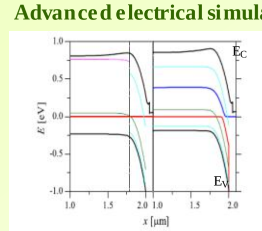

Fig. 3. Band diagrams under the initial conditions of Table 2. Left: relaxed; the black vertical line marks the transition from (predominantly) donor configuration (x<1.76 µm) to acceptor configuration (x>1.76 µm). Right: light soaked; the absorber is almost completely in the acceptor configuration. The curves shown are black: E_C, E_V; red E_F (left) or E_{Fp} (right); dark blue: E_{Fn} (right); E_{TR}: green; the two levels of the metastable acceptor configuration: light blue; the level of the metastable donor configuration: pink.

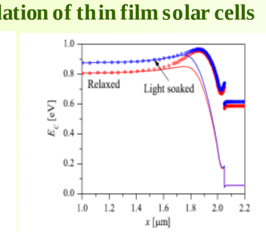

Fig. 5. The barrier in the conduction band, depending on the initial conditions (red: relaxed and blue: light soaked) and on the actual work point (solid line: dark $V=0$ and light at J_{sc} coinciding; open circles: light, at $V=V_{oc}$).

A band gap grading profile was set that results in a small but influential hump or energy barrier in the conduction band

Advanced electrical simulation of thin film solar cells

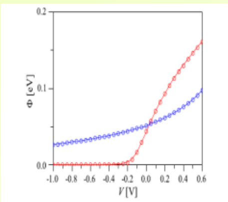

Fig. 6. Energy barriers in the conduction band as a function of applied voltage, in the relaxed (red) or light soaked state (blue). The solid line is calculated in dark, the symbols are calculated under one sun illumination.

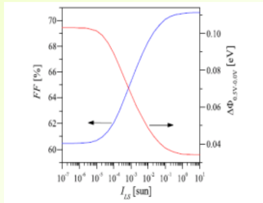

Fig. 8. Calculated fill factor FF and difference in barrier height Φ(0.5 V)−Φ(0 V) as a function of the light intensity during light soaking.

- A barrier in the CB impedes the collection of electrons that are generated in the absorber to the left of the barrier
- Results in light current reduction at FB thus affecting FF

Modeling metastabilities in chalcopyrite-based thin film solar cells
K. Decock, P. Zabierowski, and M. Burgelman, J. Appl. Phys. 111, 043703 (2012)

- The effect of voltage induced metastabilities on the capacitance-voltage characteristics of CIGS
- Defect, (V_{Se}-V_{Cu}) complex, transitioning from charged donor to charged acceptor configuration
- The agreement between the simulation and measurement results has been obtained using a simple model, and optimizing only 5 parameters
  - E_{TR}, the shallow doping density N_A, the (V_{Se}-V_{Cu}) complex density N_M, the density N_t of the additional acceptor defect and its energy E_t.

Modeling metastabilities in chalcopyrite-based thin film solar cells

Symbols represent measurement results

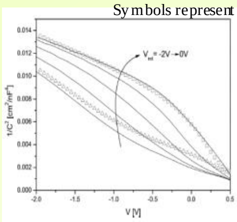

FIG. 3. Mott–Schottky plots of C-V-measurements ($T = 200$ K; $f = 1$ MHz) in the relaxed state (squares) and after reverse bias treatment (triangles). The reverse bias state was obtained by applying −2 V at 300 K for 1 h before measurement. The solid lines are the simulation results for different voltages applied during the reverse bias treatment (V_{rb}) ranging from −2 V to 0 V in steps of 0.5 V.

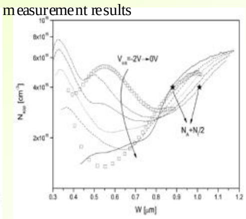

FIG. 4. Apparent defect density calculated from the C-V simulations ($T = 200$ K; $f = 1$ MHz; $V = -4$ V–0.5 V). The apparent defect density belonging to the measurement results displayed in Fig. 3 are shown using identical symbols. The stars mark the points where $N_{meas} \approx N_A + N_t/2$ and thus where $W = 2\lambda$, as will be explained in the discussion section.

Design and optimization of large area thin-film CdTe detector for radiation therapy imaging applications
E. I. Parsai, D. Shvydka, J. Kang, Med. Phys. 37 (2010) 3980

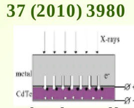

- Investigate performance of thin-film CdTe material in detecting 6MV x-rays
- The utilization of this material has become technologically feasible only in recent years due to significant development in large area photovoltaic applications
- Extensive MCNP simulations to evaluate geometrical parameters, detective quantum efficiency, scatter
- Results of absorbed energy simulation were used in device operation modeling (with SCAPS) to predict the detector output signal, and compared with measured signal

Design and optimization of large area thin-film CdTe

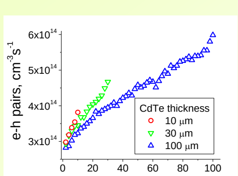

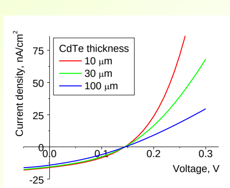

- MC modeled electron-hole generation profiles were used as input for SCAPS
- CdTe/CdS solar cell with a built-in junction field of ~10^4 V/cm; the resulting readout voltages are >100 mV for detector layers working in PV mode

Design and optimization of large area thin-film CdTe

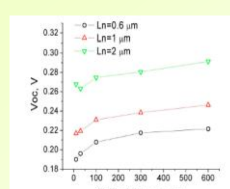

FIG. 16. Voltage output for a detector with varying CdTe thickness modeled with SCAPS for different values of the minority carrier diffusion length.

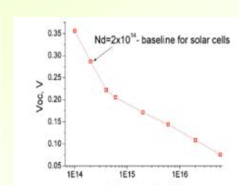

FIG. 17. Output voltage variation with defect densities for 4 μm thick CdTe detector obtained with SCAPS.

- Better quality of material results in higher readout signals
- Defect density study was only possible for the standard solar cell device thickness range (4-10μm)

Modeling the effect of 1 MeV electron irradiation on the performance of n+–p–p+ silicon space solar cells
A. Hamache, N. Sengouga, A. Meftah, M. Henini, Radiation Physics and Chemistry 123 (2016) 103–108

- Performance of cells used in space degrades after irradiation; anomalous increase in performance right before failure
- Analyzed several defects (experimentally established) which act as recombination centers and/or traps of free carriers

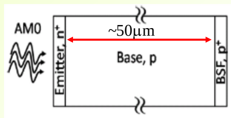

Fig. 1. A two-dimensional schematic view of the Si n+–p–p+ solar cell. The emitter is illuminated by an air mass zero spectrum (AM0) from the. BSF is the back surface field.

Table 2
The parameters of the commonly detected defects in Si solar cells irradiated by 1 MeV electrons (Yamaguchi, 2001; Yamaguchi et al., 1999b). Introduction rate, k is the proportionality factor between the trap density and the fluence ($k = N_T/\varphi$).

Activation energy (eV)	Capture cross section, σ (cm²)	Introduction rate, k (cm⁻¹)	Trap type
E_V+0.18	3.1×10^{-15}	0.002	Majority
E_V+0.36	6.2×10^{-15}	0.016	Majority
E_C−0.20	9.9×10^{-15}	0.002	Minority
E_V+0.56	6.3×10^{-13}	0.004	Majority
E_C−0.71	1.55×10^{-13}	0.004	Minority

Modeling the effect of 1 MeV electron irradiation

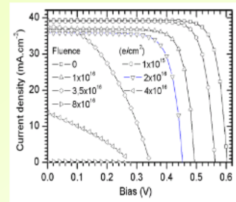

Fig. 4. The calculated J–V characteristics of the n+–p–p+ Si solar cell under AM0 for different fluences of 1 MeV electron irradiation by taking into account all the acceptor traps together with the shallower donor trap (E_C–0.20eV) only and changing the introduction rate of the latter from 0.002 to 0.04 (compare to Fig. 2

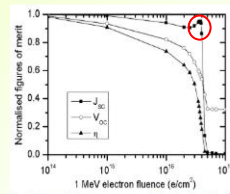

Fig. 5. The extracted short circuit current, normalized to the unirradiated value, from the calculated J–V characteristics (Fig. 4) of the n+–p–p+ Si solar cell under AM0 for different fluences of 1 MeV electron irradiation by by taking into account all the acceptor traps together with the shallower donor trap (E_C–0.20eV) only and changing the introduction rate of the latter from 0.002 to 0.04.

It was concluded that a shallower donor trap is responsible for the phenomenon while the deeper donor trap enhances this phenomenon

Summary

- SCAPS-1D is a versatile package for semiconductor device modeling
- Output for I/V, C/V, C/f, Q(λ), band diagrams, concentrations, and currents
- Data analysis for I-V, C-V, C-f
- A number of standard models available with the distribution package
- Well-developed user interface, convenient scripting facilities

References

- SCAPS manual, M. Burgelman, K. Decock, A. Niemegeers, J. Verschraegen, S. Degrave, Version: 17 february 2016
- SCAPS 3.0, An introduction, K. Decock and M. Burgelman
- M. Burgelman, P. Nollet, S. Degrave, Thin Solid Films 361 (2000) 527
- Additional references are provided within slides